Journal Pre-proof

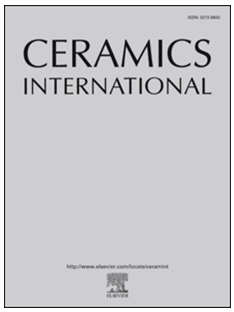

Study on the coloring mechanism of the Ru celadon glaze in the Northern Song Dynasty

Pei Shi, Fen Wang, Biao Zhang, Hongjie Luo, Jianfeng Zhu, Guiqiang Fei

PII: S0272-8842(20)31798-3

DOI: https://doi.org/10.1016/j.ceramint.2020.06.139

Reference: CERI 25566

To appear in: *Ceramics International*

Received Date: 5 June 2020

Revised Date: 11 June 2020

Accepted Date: 12 June 2020

Please cite this article as: P. Shi, F. Wang, B. Zhang, H. Luo, J. Zhu, G. Fei, Study on the coloring mechanism of the Ru celadon glaze in the Northern Song Dynasty, *Ceramics International* (2020), doi: https://doi.org/10.1016/j.ceramint.2020.06.139.

This is a PDF file of an article that has undergone enhancements after acceptance, such as the addition of a cover page and metadata, and formatting for readability, but it is not yet the definitive version of record. This version will undergo additional copyediting, typesetting and review before it is published in its final form, but we are providing this version to give early visibility of the article. Please note that, during the production process, errors may be discovered which could affect the content, and all legal disclaimers that apply to the journal pertain.

© 2020 Published by Elsevier Ltd.

Journal Pre-proof

Study on the coloring mechanism of the Ru celadon glaze in the Northern Song Dynasty

Pei Shi[a], Fen Wang[a *], Biao Zhang[a], Hongjie Luo[b], Jianfeng Zhu[a], Guiqiang Fei[c]

[a] Shaanxi Key Laboratory of Green Preparation and Functionalization for Inorganic Materials, School of Materials Science and Engineering, Shaanxi University of Science and Technology, Xi'an 710021, PR China

[b] Research Institute of Cultural Relics, Shanghai University, Shanghai 200444, PR China

[c] College of Chemistry and Chemical Engineering, Shaanxi University of Science & Technology, Xi'an 710021, PR China

Abstract

The Ru kiln is one of the five most famous kilns in the Chinese Song Dynasty. To clarify the coloring mechanism of the Ru celadon glaze, the celadon samples from the Ru Guan kiln site of Qingliangsi were analyzed by spectrophotometer, X-ray fluorescence spectrum, Raman spectroscopy, scanning electron microscopy and X-ray photoelectron spectrum. The results indicated that the molar ratios of SiO_2/Al_2O_3 and $CaO/(CaO+Al_2O_3)$ affected the formation of micro-bubbles, anorthite crystals and phase separated structures. A large number of bubbles and anorthite crystals formed special glossiness and opacifying effect in the Ru celadon glaze. And then, dense phase separation droplets in the amorphous region were in short-range order, but their diameters (31-46 nm) were too small to form visible structural colors on glaze surfaces. Only “opal effect” was formed by the light scattering, which added the aesthetic feeling for the Ru celadon. Besides, the phase separation droplets intensified the segregation of iron, and thus deepened the chemical color and made the Ru celadon glaze appear green-blue. Due to the neutral to alkaline soil at the Ru Guan kiln site, the water in the soil and its corrosion on the Ru celadon glaze resulted in the formation of Si-OH bond.

* Corresponding author: Tel.: +8602986131687; fax: +8602986168188.
Email addresses: wangf@sust.edu.cn (Fen Wang)

Keywords: Ru Guan kiln; Qingliangsi; Celadon glaze; Northern Song Dynasty; Coloring mechanism

1. Introduction

Ru kiln, located in Qingliangsi, Baofeng Country, Henan Province, is one of the five most famous kilns (Ru, Guan, Ge, Ding and Jun kilns) in the Chinese Song Dynasty (A.D. 960-1279) [1]. It started from the earlier Song Dynasty, matured in the late Northern Song Dynasty and stopped development in the late Yuan Dynasty. In the later period of the Northern Song Dynasty, from Yuanyou to Chongning for more than 20 years, Ru kiln had been making celadon for imperial courts. The best of glaze color was sky-green, and the body color was the standard of fragrant grey. In the late Northern Song Dynasty, the Ru celadon was with more fresh color and more exquisite craftsmanship. At that time, it had the reputation of “Ru kiln is the chief” [2].

The researches on the chemical composition of the Ru celadon glaze and its raw material were systematic. Ding et al. [3] found that the celadon glaze of the Ru kiln unearthed in the Ru Guan kiln site of Qingliangsi had the characteristics of high calcium and aluminum contents, which provided the physical and chemical basis for the formation of anorthite microcrystalline cluster and thick glaze layer, and created the jade-like quality of the celadon glaze. Also, fibrous and radiating aggregates with optical properties similar to agate were observed in the Ru celadon glaze by polarization microscope. It showed that the Ru celadon glaze was not only made of glaze ash and feldspar materials with relatively high aluminum content but also mixed with agate.

For coloring of the Ru celadon glaze, researchers had the same view that the glaze color was the result of the interaction of chemical color and structural color. Zhang et al. [4] investigated that the glaze color of the Ru celadon was mainly related to the concentration of structural iron ions, rather than that of the Fe_2O_3 and Fe_3O_4. As the Fe^{2+}/Fe^{3+} ratio gradually increased, the glaze color of the Ru celadon would gradually change from pea green to sky green. Li et al. [5] revealed that the Ru celadon glaze belonged to crystalline and phase separation glaze for the first time. A dual coloring mechanism was in effect for the Ru celadon glaze, covering chemical

Journal Pre-proof

compositional coloring by iron ion chromophore and structural coloring by structural inhomogeneities including nano-sized phase separation structures and micro-sized crystals, bubbles and inclusions. Yang et al. [6] confirmed the study of Li et al. and indicated that there were amount of crystallites and phase separation structures in the Ru celadon glaze, the former met Mie scattering conditions and the latter met Rayleigh scattering conditions. Nevertheless inspired by structural colors of amorphous arrays in the biological world, Yin et al. [7] proposed the phase-separated structures with short-range order could form the structural color in the glaze for the first time. It was the physical origin of opalescence blue in the Ru celadon glaze. However, until now, few studies have been made to interpret the relationship between composition and structure-property and to explore the coloring mechanism of the Ru celadon glaze.

In this paper, the apparent performance, chemical composition, microstructure and chemical state of iron ions of Ru celadon glazes with different colors were compared, and the main factors affecting the appearance of Ru celadon glaze were studied. In addition, the interaction between the chemical color and the structural color, as well as the internal relationship between them and the glaze color were analyzed. Based on these, the color mechanism of the Ru celadon glaze in the Northern Song Dynasty was revealed comprehensively and systematically.

2. Experimental

2.1 Information about the samples

All of the samples excavated from the Ru Guan kiln site of Qingliangsi, kindly loaned by the Palace Museum in Beijing. The photos and information of the samples were shown in Fig. 1 and Table 1.

2.2 Methodology

The glaze color of samples was analyzed by spectrophotometer (X-Rite Ci7800, America). The measuring aperture was 6 mm. The chemical composition were tested by X-ray fluorescence (XRF, XGT-7200V, Japan) with Rh target. The molecular structure of the glass phase was studied by confocal Raman spectroscopy (Raman, Renishaw-invia, England). The laser wavelength was 532 nm, and the laser power

Journal Pre-proof

was 3.35 mW. And then, the crystalline phases were identified by X-ray diffraction (XRD, D/max 2200PC, Japan) with Cu K_α radiation (λ=1.5406 Å) under 40 kV and 100 mA. The scanning speed was 8º/min and the step degree was 0.02º. Microstructure and phase compositions were performed by using scanning electron microscopy (SEM, S4800, Japan) equipped with an energy dispersive spectrometry (EDS). Before the testing, the surfaces of samples were etched in 1 vol% HF for 40 s to expose the crystals and phase separation structures, and then sprayed platinum to make the glaze surfaces conductive. Finally, the valence and coordination state of iron ions in the glaze were analyzed by ultraviolet-visible-NIR (UV-vis-NIR) spectrometer (Cary 5000, America) and X-ray photoelectron spectrum (XPS, VG Scientific, England) with Al K_α radiation.

3. Results and discussion

3.1 Relationship between chemical composition and apparent performance

Table 2 and Fig. 2 show the colorimetric values (L*, a*, b*, C*, h*) of samples and the corresponding scatter diagrams of L*, C* and h*. From Fig. 2 (a), L* values of all samples were between 56 and 66, and increased in the order of R1, R3, R2 and R4. From Fig. 2 (b), the glaze colors of samples were located in the yellow-green-blue area and close to the green axis. By comparing h* of samples, the green-blue tone of samples decreased in the order of R2, R1, R4 and R3. Due to the small difference in body colors of the samples, their glaze colors were mainly determined by the chemical composition, microstructure and the content of different valence iron ions.

Table 3 presents the glaze compositions of these samples. The content of SiO_2 changed obviously, from 70.65 wt% to 75.24 wt%. Next were Al_2O_3 and CaO with contents of 11.56-14.79 wt% and 6.52-8.26 wt%, respectively. And the difference of the Fe_2O_3 content was not huge. Also, the samples contained 1.49-2.71 wt% $MgO+P_2O_5+MnO_2$, indicating that a certain amount of plant ash was used as a flux for the Ru celadon glaze [8]. The research showed that 0-3 wt% P_2O_5 in the chemical composition helped the green-blue color of the celadon glaze [9]. Hence, P_2O_5 in the Ru celadon glaze could promote the glaze color to be green-blue.

Based on Table 3, the discriminant coefficient b ($RO/(RO+R_2O)$) of the calcium

Journal Pre-proof

glaze and the molar ratios of $CaO/(CaO+Al_2O_3)$ and SiO_2/Al_2O_3 were calculated, as shown in Table 4. The b values of samples were between 0.83 and 0.90. The results showed that the Ru celadon glaze in the Northern Song Dynasty belonged to the calcium glaze, and the selection and proportion of raw materials were relatively stable [10]. Owing to the largest mole ratio of $CaO/(CaO+Al_2O_3)$, R4 had the strongest glossiness than others [11]. Moreover, comparing the mole ratio of SiO_2/Al_2O_3, R1 was similar to R2, while R3 and R4 were also similar.

Fig. 3 is the optical images on the glaze surfaces of samples. There were many bubbles in the glazes, whereas their sizes were different. The bubble sizes of R1 and R2 were larger than those of R3 and R4. Zhang et al. [12] investigated that when the mole ratio of $CaO/(CaO+Al_2O_3)$ was more than 0.4 and less than 0.6, the viscosity of glass melt increased with the increase of SiO_2 content. From Table 4, the mole ratios of $CaO/(CaO+Al_2O_3)$ for all samples were in this range, so their viscosity met to the change rule of SiO_2 content. With higher SiO_2 content, the viscosity of glaze melt would be higher, as well as the movement and aggregation of bubbles would also get more difficult. As a result, the bubble size in the R1 and R2 was large and the number was few. The dense bubbles in the R3 and R4 glazes promoted the scattering of the incident light, causing that the glaze surfaces appeared glossy and opacifying effects.

3.2 Effect of microstructure on *apparent performance*

Fig. 4 (a) presents the Raman spectra on glaze surfaces of samples in uniform and non-crystalline areas. In the range of 150-1250 cm^{-1}, all samples had two Raman peaks in 483.6 cm^{-1} and 1031.4 cm^{-1}, which corresponded to the Si-O bending and stretching vibrations in the $[SiO_4]$ tetrahedron, respectively [13, 14]. Phillippe et al. [14] investigated that the degree of polymerization fixed by the content of fluxing ions breaking the Si–O bonds determined the relative intensity of the Si–O bending and stretching vibrations ($Ip=A_{500}/A_{1000}$). The area ratio of these bending and stretching vibration peaks was well correlated to the glass composition (the ratio of fluxing oxide/network-forming oxide). This last ratio was directly related to the melting temperature. Therefore, the firing temperature of the ceramic glaze could be determined indirectly by comparing the Ip values of Raman spectra of different

samples. The larger the Ip value was, the higher the firing temperature was. These two Raman peaks were fitted by a Gaussian function, and the corresponding Ip values were calculated, as shown in Figure 4 (b). The Ip values of the samples were in the range of 0.5-0.7, and increased in the order of R3, R1, R4 and R2, so the firing temperatures of samples also increased in the same order.

In addition, from Fig. 4 (a), the samples had two Raman peaks at 3604.7 cm^{-1} and 3850.0 cm^{-1}, which was caused by the stretching vibration of -OH in the Si-OH bond [15]. Research shows that the soil in the Ru Guan kiln site of Qingliangsi is brown soil with alkalescence [16]. Since the ancient ceramic was buried underground for several years, the glass phase in the glaze was corroded by the moisture in the soil and itself, and the Si-O-R bond and Si-O-Si bond were destroyed, forming the Si-OH bond. The corrosion process continued without being controlled by diffusion. The chemical reaction equations were shown below:

$$Si{-}O{-}R + H{-}OH \rightarrow Si{-}OH + R^{+} + OH^{-} \quad (1)$$

$$Si{-}O{-}Si + OH^{-} \rightarrow Si{-}OH + Si{-}O{-} \quad (2)$$

In addition to the corrosive media, the corrosion of glass is closely related to the porosity and microstructure. The higher the firing temperature and the higher the chemical stability of the glaze, the stronger the corrosion resistance of the glass phase. Therefore, the intensity of the stretching vibration peak of -OH was opposite to the firing temperature of the sample and decreased in the order of R3, R1, R4 and R2.

Fig. 5 shows the XRD spectrums on the glaze surfaces of samples. The diffraction intensity was weak, indicating the poor crystallization property of all the samples. The characteristic amorphous hump could be seen within the $2\theta \approx 15\text{-}35°$ range in the samples, which were associated with a large amount of aluminosilicate glass. Meanwhile, some weak crystallization peaks, corresponding to anorthite ($CaAl_2Si_2O_8$, PDF#41-1486), quartz (SiO_2, PDF#47-1144) and clinoptilolite-Na ($(Na,K,Ca)_5Al_6Si_{30}O_{72}\cdot 18H_2O$, PDF#47-1870) crystallizations, were also detected in every sample. By comparison, the diffraction peak intensities of anorthite in R1 and R2 were stronger, while those of quartz in R3 and R4 were stronger, which was related to the molar ratios of $CaO/(CaO+Al_2O_3)$ and SiO_2/Al_2O_3 in the samples. From

the phase diagram of CaO-Al_2O_3-SiO_2 system, it was conducive to the precipitation of quartz when the molar ratios of $CaO/(CaO+Al_2O_3)$ and SiO_2/Al_2O_3 were larger, and the smaller the molar ratio, the better the precipitation of anorthite crystals [5].

Fig. 6 displays SEM micrographs on the glaze surfaces of samples etched by HF acid and EDS spectra of long columnar crystals. As can be seen from the SEM micrographs, some long columnar crystals and phase-separated structures were exposed to the glaze surfaces. For R1 and R2, they were independent of each other. However, the phase separation structure in R3 and R4 was closely distributed around the crystal. From the EDS spectra, these crystals were rich in Ca, Al and Si. Combining XRD and EDS results, it was determined that the long columnar crystal was anorthite. According to the research from García et al. [17], there were three necessary conditions for the formation of Mie scattering. First of all, dielectric particles were spherical or nearly spherical. And then, they are monodisperse. Thirdly, the average diameter of scattering particles was more than 200 nm. Based on the above conditions, it was determined that the anorthite crystals in the Ru celadon glaze could not form Mie scattering.

During the firing process, with the precipitation and growth of anorthite crystals, Al_2O_3 in the surrounding glass phase is consumed in large amounts. With the sharp increase of the SiO_2/Al_2O_3 molar ratio, the chemical composition of the glass phase rapidly shifts to the liquid-liquid immiscibility region. When the firing temperature exceeds 950 °C, the phase-separated structure occurs in the glass phase. Since the molar ratios of SiO_2/Al_2O_3 in the R3 and R4 were larger than that of R1 and R2, the anorthite crystals in them were more easily formed accompanying the phase-separated structure and were closely distributed around the crystals. Due to low content and uneven distribution, the structural color could not be formed by these phase-separated structures. Although the presence of crystalline region did not form structural colors, it greatly improved the opalescence of the Ru celadon glaze.

3.3 Analysis of the coloring mechanism

In addition to the high molar ratio of SiO_2/Al_2O_3, the introduction of phosphorus into silicate glass could not only reduce the liquidus temperature and viscosity, but

also promote the formation of phase separation structures on a wide scale [18]. In the chemical composition of samples, the molar ratios of SiO_2/Al_2O_3 were 8.233-11.065, and they contained 0.39-0.63 wt% P_2O_5, so that the phase-separated structure was distributed throughout the amorphous region. The enlarged figures of the glass phase in Fig. 6 were shown in Fig. 7. The discrete droplet phase-separated structures were formed in the samples, and their average diameters were 31, 35, 40 and 46 nm, respectively. Yasumoli [19] analyzed the influence of the Al_2O_3 content on the phase-separated structure in the $CaO-Al_2O_3-SiO_2$ ternary glass system. With the increase of Al_2O_3 content, the size of phase separation droplets decreased, from micro nano size to nano size. This was because the introduction of Al_2O_3 improved the mutual solubility of calcium-rich phase and silicon-rich phase.

The insets in Fig. 7 were the 2D-FFT images corresponding to the phase-separated structures. There were a circular ring around the origin, indicating that the phase separation droplets of the samples were in short-range order rather than complete disorder. Whereas, their average sizes were not within the range of 106-348 nm, so the amorphous structural color formed in the samples was weak. However, the phase-separated structure could lead to the aggregation or segregation of iron, further deepening the chemical color of the Ru celadon glaze [20].

Based on the above results, the chemical color of iron element played an important role in the Ru celadon glaze. Fig. 8 (a) shows the UV-vis-NIR absorption spectra of the samples, showing five absorption peaks at 269 nm, 875 nm, 1168 nm, 1418 nm and 1943 nm, respectively. Fe^{3+} in $[FeO_4]$ tetrahedron presented an intense charge transference peak around 269 nm [21]. And the peak at 875 nm associated to the characteristic absorption of Fe^{3+}-O-Fe^{2+} [22]. Besides, there were two strong absorption peaks at 1168 and 1943 nm in the samples. They corresponded to the characteristic absorption peaks of Fe^{2+} in $[FeO_6]$ octahedron and $[FeO_4]$ tetrahedron, respectively. The shoulder peak at 1419 nm was related to the deformation of $[FeO_6]$ octahedron structure of Fe^{2+} [23]. Furthermore, for R3 and R4, the characteristic absorption peak of Fe^{3+} was stronger than that of R1 and R2, while the characteristic peak of Fe^{2+} was relatively weaker. And R2 had the strongest characteristic peak

Journal Pre-proof

intensity of Fe^{3+}-O-Fe^{2+}. In general, the tetrahedral coordination of Fe^{3+} makes the glass yellow-green, while Fe^{2+} and Fe^{3+}-O-Fe^{2+} make the glass bluish green [21]. Therefore, the color of Ru celadon glaze was closely related to the valence of iron ions.

In order to further prove the relationship between the glaze color of Ru celadon and the valence state of iron ions, XPS was used to analyze the chemical state of iron ions in the samples. Figure 8 (b) shows the XPS fitting pattern of the Fe2p3/2 on the sample surfaces. Two peaks at 709-711 eV and 714-715 eV were observed, which were ascribed to Fe 2p3/2(II) and Fe 2p3/2(III) [24]. According to the relative areas of the peaks, the atomic ratios of Fe^{2+} and Fe^{3+} in the four samples were 57.41/42.59, 66.37/33.63, 42.26/57.74 and 46.71/53.29, which was consistent with the results of UV-vis-NIR absorption spectra.

In the Northern Song Dynasty, the green stone and red stone were used as raw materials of the Ru celadon glaze [3], and the XRD spectrums were shown in Fig. 9. The main crystals had quartz (SiO_2, PDF#48-1045), calcite ($CaCO_3$, PDF#47-1743), montmorillonite-15A ($Ca_{0.2}(Al,Mg)_2Si_4O_{10}(OH)_2 \cdot 4H_2O$, PDF#13-0135), muscovite-3T ($(K,Na)(Al,Mg,Fe)_2(Si_{3.1}Al_{0.9})O_{10}(OH)_2$, PDF#07-0042) and minor kaolinite ($Al_2Si_2O_5(OH)$, PDF#14-0164), which provided iron through muscovite-3T and impurity minerals of iron from clay minerals. The firing temperature, firing atmosphere and acid-base property of basic glaze had influences on the valence state of iron. High temperature, strong acid and reducing atmosphere contributed to the reduction of Fe^{3+}, and low temperature, strong alkali and oxidizing atmosphere contributed to the oxidation of Fe^{2+} [25]. It was because of these that lead to the differences of glaze color of the Ru celadon in the Northern Song Dynasty.

4. Conclusion

The composition and structural characteristics of the Ru celadon glaze in the Northern Song Dynasty were studied, besides the coloring mechanism was analyzed systematically. The results were as follows:

(1) In the Ru celadon glaze of the Northern Song Dynasty, the molar ratios of SiO_2/Al_2O_3 and $CaO/(CaO+Al_2O_3)$ affected the formation of micro-bubbles, anorthite

crystals and phase separated structures. A large number of bubbles and anorthite crystals formed special glossiness and opacifying effect.

(2) Although the phase-separated droplets in the amorphous region had short-range order, due to their high density and particle size of only 31-35 nm, the resulting structural color was weak. However, the opal effect could be formed by scattering of phase separation structures, which added to the unique beauty of Ru celadon.

(3) The green-blue tone of the Ru celadon glaze was mainly determined by the contents of Fe^{2+} and Fe^{3+}-O-Fe^{2+}. Also, the phase-separated droplets aggravated the segregation of iron, thus deepened the chemical color, and further made the Ru celadon glaze appear green-blue.

(4) Due to the neutral to alkaline soil at the Ru Guan kiln site of Qingliangsi, the moisture in the soil and its corrosion caused the formation of Si-OH bond. The lower the firing temperature, the stronger the Si-OH bond. It could be used for the identification of Ru kiln celadon.

ACKNOWLEDGEMENTS

This work was supported by the National Natural Science Foundation of China (51972201), National Key Technologies R & D Program of China (2019YFC1520300) and the Shaanxi Science & Technology Co-ordination & Innovation Project, China (2017TSCXL-GY-07-05, 2017TSCXL-GY-08-05).

References

[1] W.D. Li, J.Z. Li, Z.Q. Deng, J. Wu, J.K. Guo, Study on Ru ware glaze of the Northern Song dynasty: One of the earliest crystalline-phase separated glazes in ancient China, Ceram. Int. 31 (2005) 487-494.

[2] B. Zhang, H.S. Cheng, W.J. Zhao, Z.Y. Gao, G.X. Li, J.Z. Xie, M. Guo, F.J. Yang, PIXE analysis of Chinese Ru celadon made in the 11-12th centuries, X-ray Spectrom. 35 (2006) 27-32.

[3] Y.Z. Ding, H. Li, X.M. Sun, T.M. Chen, J.M. Miao, Technical discussion on celadon glaze of Ru Guan kiln in Qingliangsi, Chn. Cult. Herit. Sci. Res. (2017) 54-62.

Journal Pre-proof

[4] B. Zhang, Z.Y. Gao, W.J. Zhao, G.X. Li, H.S. Cheng, Z.Q. Zhang, Mössbauer spectroscopy and neutron activation analysis of ancient Chinese glazes, Appl. Clay Sci. 25 (2004) 161-165.

[5] W.D. Li, J.Z. Li, Z.Q. Deng, J. Wu, J.K. Guo, Study on Ru ware glaze of the Northern Song dynasty: One of the earliest crystalline-phase separated glazes in ancient China, Ceram. Int. 31 (2005) 487-494.

[6] Y.M. Yang, M. Feng, X. Ling, Z.W. Mao, C.S. Wang, X.M. Sun, M. Guo, Microstructural analysis of the color-generating mechanism in Ru ware, modern copies and its differentiation with Jun ware, J. Archaeol. Sci. 32 (2005) 301-310.

[7] H.W. Yin, Study on the coloring mechanism and preparation method of structural color, Fudan University, Shanghai, 2008.

[8] J.Y. Shen, H. Julian, Chemical composition and raw materials of Yaozhou celadon glaze from the Tang to Northern Song Dynasties, Western Archaeol. (2018) 232-241.

[9] J.F. Zhu, P. Shi, F. Wang, T. Zhao, H. Jiang, Effects of microstructure on the sky-green coloring imitating ancient Jun glazes, J. Ceram. Soc. Jpn. 124 (2016) 229-233.

[10] H.J. Luo, J.Z. Li, L.M. Gao, Classification standard of calcium glaze types in ancient Chinese ceramic and its application in glaze research, Bull. Chin. Ceram. Soc. (1995) 50-53.

[11] T.C. Ma, Ceramics technology, China Light Industry Press, Beijing, 2011.

[12] Z.W. Zhang, Z.Y. Wang, Q.F. Liang, X.H. Guo, G.S. Yu, Z.H. Yu, Analysis and prediction of the viscosity of the SiO_2-Al_2O_3-CaO ternary system in completely molten state, Chin. Soc. for Elec. Eng. 28 (2008) 39-43.

[13] P. Colomban, G. Sagon, X. Faurel, Differentiation of antique ceramics from the Raman spectra of their coloured glazes and paintings, J. Raman Spectrosc. 32 (2001) 351-360.

[14] P. Colomban, O. Paulsen, Non-destructive determination of the structure and composition of glazes by Raman spectroscopy, J. Am. Ceram. Soc. 88 (2005) 390-395.

[15] B.Q. Lu, L.J. Qi, Y.B. Xia, Study on the vibration spectra of nephrite cat's eye

from Sichuan Province, Shanghai Geol. 29 (2008) 57-60.

[16] F. Yang, Study on building and application of Henan province soil database, Henan Agricultural University, Zhengzhou, 2008.

[17] P.D. García, R. Sapienza, J. Bertolotti, M.D. Martín, Á Blanco, A. Altube, L. Viña, D.S. Wiersma, C. López, Resonant light transport through Mie modes in photonic glasses, Phys. Rev. A 78 (2008) 023823.

[18] B. Zhang, J.F. Zhu, P. Shi, F. Wang, J.H. Wang, R. Zhao, Achieving tunable sky-blue copper glaze and coloring mechanism by the introduction of phosphorus, J. Eur. Ceram. Soc. 39 (2018) 1925-1931.

[19] A. Yasumori, Preparation of functional glasses and glass ceramics using stable immiscibility, J. Ceram. Soc. Jpn. 121 (2013) 471-479.

[20] P. Shi, F. Wang, J.F. Zhu, H.B. Yang, Y. Wang, Y. Fang, B. Zhang, J.H. Wang, Amorphous photonic crystals and structural colors in the phase separation glaze, J. Eur. Ceram. Soc. 38 (2018) 2228-2233.

[21] F. Chen, L.H. Wu, E.L. Zhao, Introduction of colored glasses, Chemical Industry Press, Beijing, 2008.

[22] C.W. Zhang, The structural analysis and coordination discussion on iron-ion tinting principle in iron oxide containing glass, Glass Enamel 32 (2004) 38-46.

[23] S.G. Wang, J.J. Han, M.Q. Gao, The application of ligand field theory on the analysis of chemical states of iron in glass, Glass 6 (2000) 1-3.

[24] T. Yamashita, P. Hayes, Analysis of XPS spectra of Fe^{2+} and Fe^{3+} ions in oxide materials, Appl. Surf. Sci. 254 (2008) 2441-2449.

[25] Y. Wang, S.H. Yu, J.J. Chu, D.K. Chen, J. Chen, Study on the copper and iron coexisted coloring glaze and the mechanism of the fambe, J. Eur. Ceram. Soc. 38 (2018) 3681-3688.

Journal Pre-proof

Journal Pre-proof

Figure Captions

Journal Pre-proof

Journal Pre-proof

Table 1

No.	Body color	Thickness of glaze	Glaze appearance
R1	Gray-white	511 μm	Matte glaze surface, fine and dense cracks, sky-blue glaze
R2	Gray-white	532 μm	Bright and fine glaze surface, full of cracks, sky-blue glaze
R3	White-gray	451 μm	Bright glaze surface, green-yellow glaze
R4	White-gray	693 μm	Bright and fine glaze surface, sparse cracks, sky-green glaze

Table 2

No.	L*	a*	b*	C*	h*
R1	56.56	-6.00	2.44	6.48	157.90
R2	61.95	-5.30	-0.03	5.30	180.30
R3	60.39	-3.43	5.55	6.53	121.71
R4	65.17	-6.50	5.05	8.23	142.14

Table 3

No.	Na_2O	MgO	Al_2O_3	SiO_2	K_2O	CaO	TiO_2	Fe_2O_3	P_2O_5	MnO_2
R1	0.02	1.97	14.08	70.65	2.58	8.26	0.16	1.54	0.63	0.11
R2	0.37	2.00	14.79	71.63	2.44	6.52	0.13	1.48	0.52	0.12
R3	0.35	0.93	12.27	74.35	1.90	7.59	0.18	1.87	0.39	0.17
R4	0.10	1.09	11.56	75.24	1.82	8.24	0.11	1.20	0.52	0.12

Table 4

No.	R1	R2	R3	R4
b ($RO/(RO+R_2O)$)	0.876	0.839	0.860	0.893
$CaO/(CaO+Al_2O_3)$	0.517	0.445	0.530	0.561
SiO_2/Al_2O_3	8.530	8.233	10.301	11.065

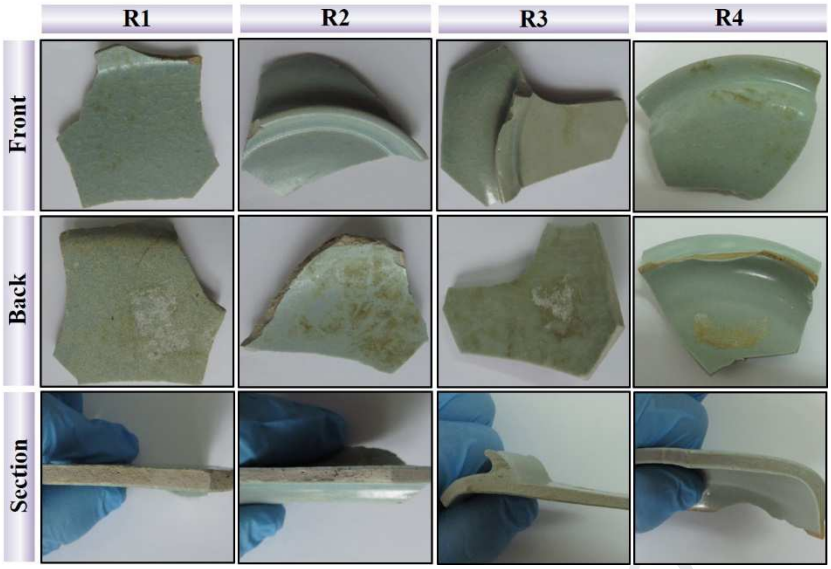

Fig. 1

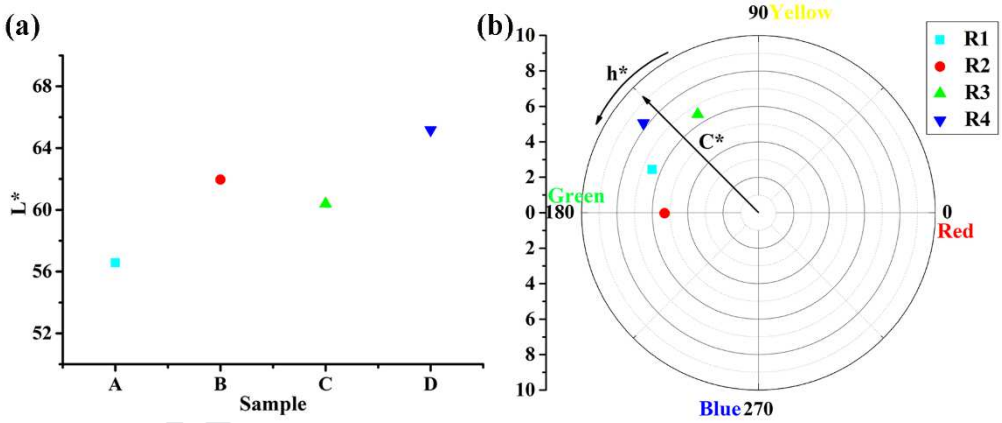

Fig. 2

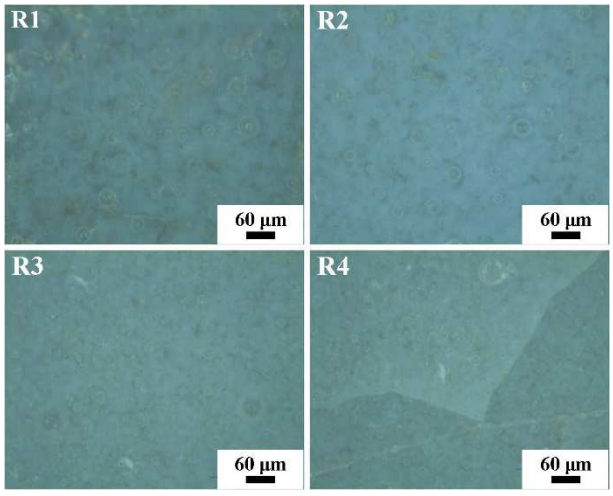

Fig. 3

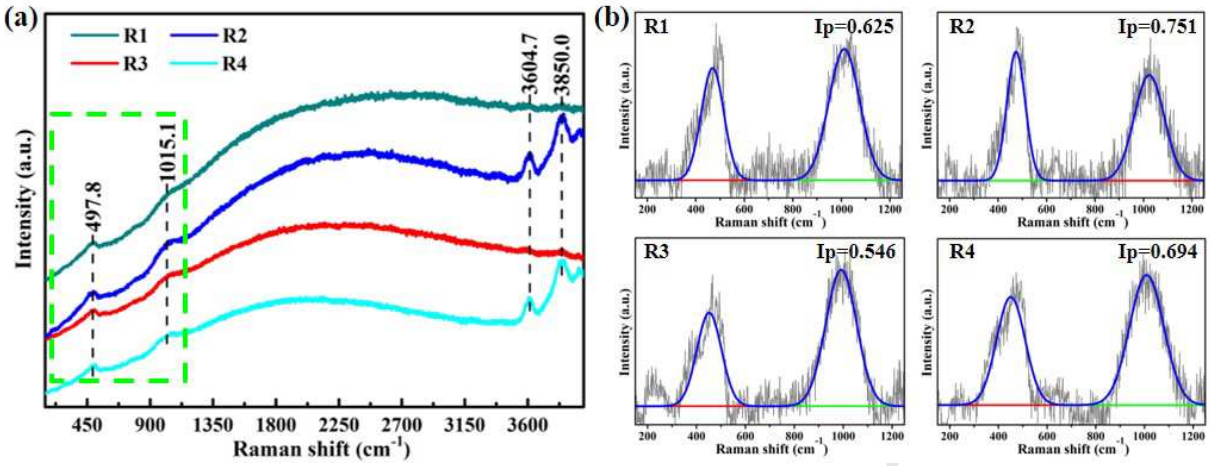

Fig. 4

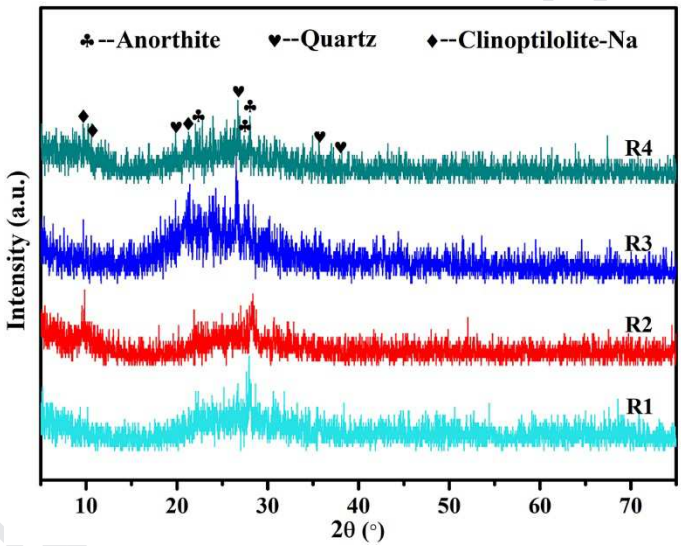

Fig. 5

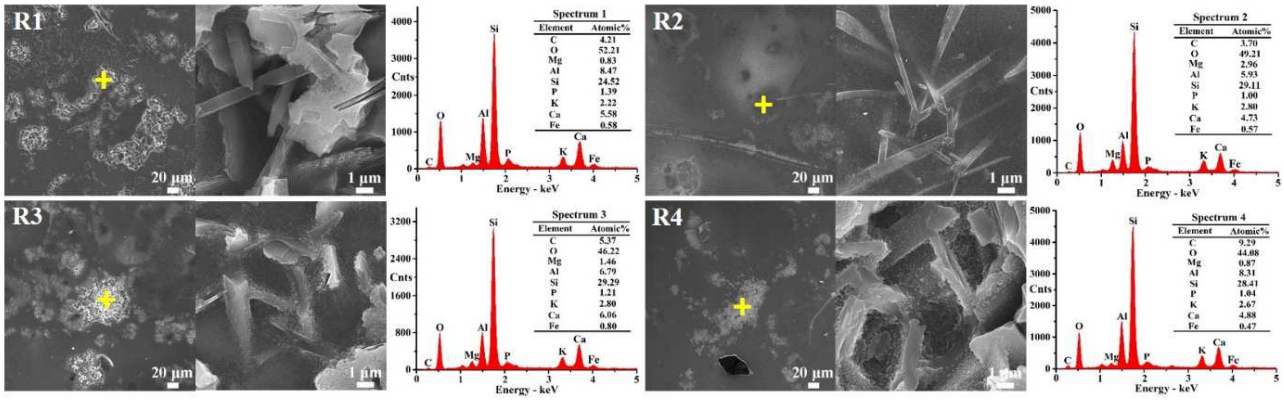

Fig. 6

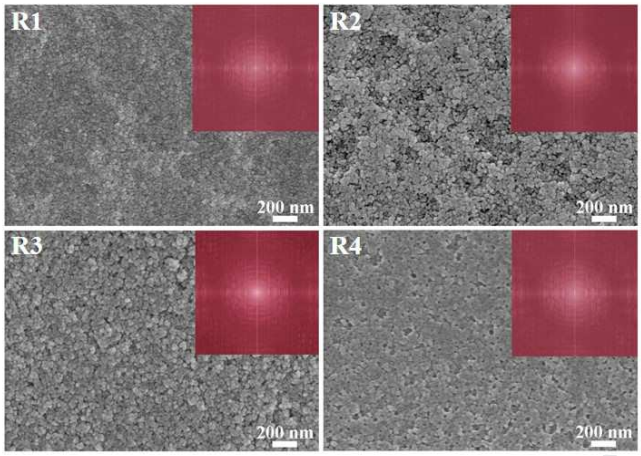

Fig. 7

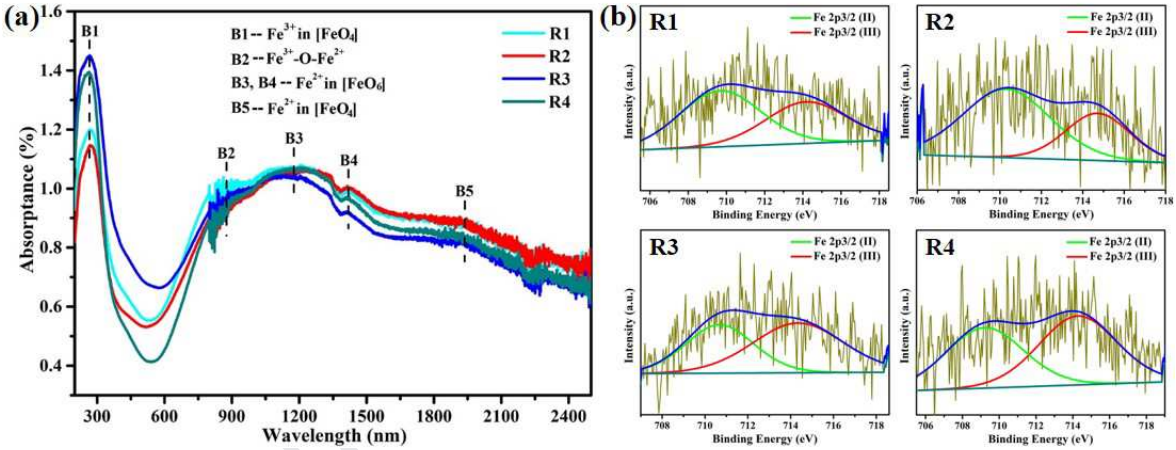

Fig. 8

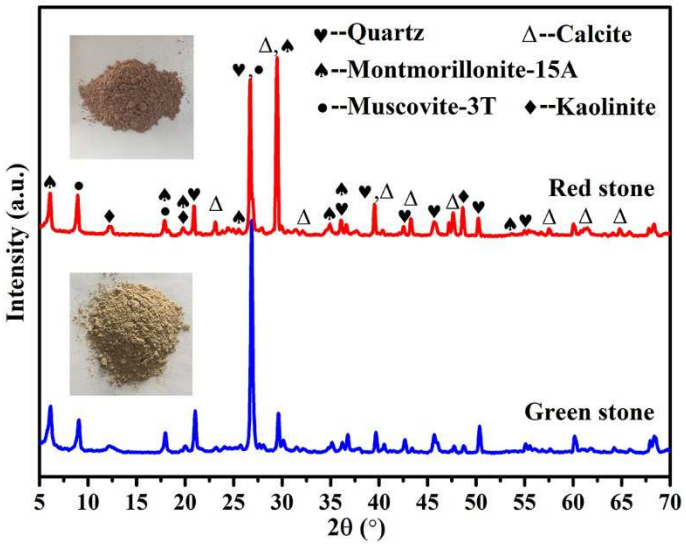

Fig. 9

Journal Pre-proof

Declaration of interests

☐ √ The authors declare that they have no known competing financial interests or personal relationships that could have appeared to influence the work reported in this paper.

☐The authors declare the following financial interests/personal relationships which may be considered as potential competing interests:

Journal Pre-proof